

Influence of pregnancy stage and fetus position on the whole-body and local exposure of the fetus to RF-EMF

This content has been downloaded from IOPscience. Please scroll down to see the full text.

2014 Phys. Med. Biol. 59 4913

(<http://iopscience.iop.org/0031-9155/59/17/4913>)

View [the table of contents for this issue](#), or go to the [journal homepage](#) for more

Download details:

This content was downloaded by: nvarsier

IP Address: 193.49.124.107

This content was downloaded on 25/08/2014 at 12:46

Please note that [terms and conditions apply](#).

Influence of pregnancy stage and fetus position on the whole-body and local exposure of the fetus to RF-EMF

N Varsier^{1,2}, S Dahdouh^{2,3}, A Serrurier^{3,4}, J-P De la Plata^{3,5},
J Anquez^{3,6}, E D Angelini^{2,3}, I Bloch^{2,3} and J Wiart^{1,2}

¹ Orange, Issy les Moulineaux, France

² WHIST Joint Laboratory between Institut Mines-Telecom and Orange, France

³ Institut Mines-Telecom, Telecom ParisTech, CNRS LTCI, Paris, France

⁴ Institute of Medical Informatics, Aachen, Germany

⁵ InSimo, Strasbourg, France

⁶ Theraclion, Malakoff, France

E-mail: nadege.varsier@orange.com

Received 30 January 2014, revised 24 June 2014

Accepted for publication 15 July 2014

Published 7 August 2014

Abstract

This paper analyzes the influence of pregnancy stage and fetus position on the whole-body and brain exposure of the fetus to radiofrequency electromagnetic fields. Our analysis is performed using semi-homogeneous pregnant woman models between 8 and 32 weeks of amenorrhea. By analyzing the influence of the pregnancy stage on the environmental whole-body and local exposure of a fetus in vertical position, head down or head up, in the 2100 MHz frequency band, we concluded that both whole-body and average brain exposures of the fetus decrease during the first pregnancy trimester, while they advance during the pregnancy due to the rapid weight gain of the fetus in these first stages. From the beginning of the second trimester, the whole-body and the average brain exposures are quite stable because the weight gains are quasi proportional to the absorbed power increases.

The behavior of the fetus whole-body and local exposures during pregnancy for a fetus in the vertical position with the head up were found to be of a similar level, when compared to the position with the head down they were slightly higher, especially in the brain.

Keywords: fetus, radiofrequency, electromagnetic field, exposure

(Some figures may appear in colour only in the online journal)

1. Introduction

Over the past 30 years wireless communication systems, such as mobile phones, have been increasingly used. The versatile use of new “smartphones” and the development of small communication systems are strengthening this tendency. In spite of the existing protection limits, there is worldwide public concern about the possible health effects linked to electromagnetic field (EMF) exposure. Many questions are raised, particular for fetuses and pregnant women. The WHO has recommended the study of fetus EMF dosimetry as a high-priority research topic. However, the estimation of fetus radiofrequency (RF) exposure induced by wireless communication systems is highly complex because the exposure depends on many parameters (source, usage, frequency, posture, age of fetus). So far, few studies have been published that have analyzed the exposure of the fetus versus the pregnancy stage or the fetus position because the lack of anatomically correct models (MRI based or Ultrasonic based) of pregnant women and fetuses is a major challenge for the assessment of RF-EMF exposure.

In (Nagaoka *et al* 2008a), the authors analyzed the influence of the pregnancy stage on the whole-body and they averaged the exposure of the fetus to RF-EMF using 12, 20 and 26 weeks pregnant woman models. But fetus models at 12 and 20 pregnancy weeks were only morphed models derived from a 26 weeks pregnancy fetus model, which may not be realistic since the rate of development is variable and organ specific. In (Dimbylow *et al* 2009), the influence of the pregnancy stage was limited to three stages of pregnancy between 13 and 38 weeks, and to the averaged maximum Specific Absorption Rate (SAR) over 10 g in the fetus. The aim was to compare values with the International Commission on Non-Ionizing Radiation Protection (ICNIRP) reference levels but not to specifically analyze the influence of the pregnancy stage on exposure. In (Hadjem *et al* 2010), the aim was to specifically analyze the influence of the pregnancy stage on the whole-body exposure. This study did not include fetus models at the second trimester of pregnancy and the used models were not from the same fetus at different pregnancy stages but instead came from different fetuses modeled from segmentation of ultrasound or MR images.

To analyze the influence of the pregnancy stage on the fetus whole-body and local exposure to RF-EMF, we developed a synthetic semi-homogeneous pregnant woman model within the range 8 to 32 weeks amenorrhea (WA), using a fetus growth modeling tool between 14 and 32 WA in order to perform the analysis for the same fetus in the same position during the whole pregnancy. In the range from 8 to 13 WA, we used fetus models generated using ultrasound images (Dahdouh *et al* 2013, Anquez *et al* 2013). For pregnancy stages beyond 14 WA, we used a model combining growth modeling and segmentation of Magnetic Resonance (MR) images, allowing for the generation of utero fetal units (UFUs) within the range of 14 to 32 WA; the fetus keeping the exact same position through the whole pregnancy (Serrurier *et al* 2013, Dahdouh *et al* 2014). These UFUs were inserted in a synthetic semi-homogeneous woman body envelope in order to build pregnant woman models at different pregnancy stages (De la Plata Alcalde *et al* 2010). The fetus being positioned freely by the user, this modeling tool allowed us to analyze the influence of the fetus position on its whole-body and local exposure to RF-EMF (Serrurier *et al* 2013, Dahdouh *et al* 2014).

Section 2 presents the pregnant woman models built for the study as well as the setup of the fetal exposure to EMF. In section 3, we focus on the results of the analysis of the exposure of the fetus to EMF throughout a whole pregnancy. We will also analyze the influence of the fetus position on the whole-body and the local exposure of the fetus. These results are finally discussed and we conclude in section 4. A companion paper describes the growth modeling tool and the methods used to generate pregnant woman models that are the basis of the dosimetry analysis presented here (Dahdouh *et al* 2014).

2. Material and methods

In order to analyze the influence of the pregnancy stage on the fetus exposure to RF-EMF throughout the whole pregnancy, we developed 13 pregnant woman models from 8 to 32 WA, with 2–3 weeks increments between successive models. From 8 to 13 WA, UFUs were obtained from segmentation of ultrasound images (Dahdouh *et al* 2013, Anquez *et al* 2013) whereas from 14 to 32 WA they were generated using a fetus growth modeling tool and segmented 3D MR images (Serrurier *et al* 2013, Dahdouh *et al* 2014), which allowed us to perform our analysis by keeping the same fetus in the same position throughout almost the whole pregnancy. Considering that, during the first trimester of the pregnancy, the embryo is very small, it was reasonable to include in our study 8 to 13 WA models, even if they are not generated from the growth modeling tool.

The 13 UFUs were inserted in a synthetic semi-homogeneous woman body envelope that has been validated for dosimetry studies on the fetus exposure considering a far-field exposure (De la Plata Alcalde *et al* 2010, Jala *et al* 2013), which will be explained next.

2.1. Pregnant woman models

2.1.1. A synthetic semi-homogeneous pregnant woman model. Whole-body numerical models of heterogeneous pregnant women are very difficult to generate because obstetric images (ultrasound or MR) are never whole-body images. The easiest way to develop a full body pregnant woman model is to insert UFUs in a non-pregnant body envelope. Few numerical heterogeneous pregnant woman models exist and those that do exist were used for EMF exposure studies (Dimbylow 2006, Xu *et al* 2007, Nagaoka *et al* 2007, Nagaoka *et al* 2008b, Becker *et al* 2008). These models are, however, very specific to the fetus inserted inside the model. To have the flexibility required to develop as many pregnant woman models as are needed, we have used a synthetic semi-homogeneous woman body envelope and a physics-based modeling tool that allows us to insert any UFU inside the synthetic woman (De la Plata Alcalde *et al* 2010). The tool was developed in the framework of the ANSES project FEMONUM (<http://femonum.telecom-paristech.fr/>) and the JST-ANR project FETUS (<http://whist.institut-telecom.fr/fetus/>).

This tool allows us to control the abdominal fat layer thickness on the synthetic woman envelope. For our analysis, we chose to work with an intermediate morphology, so that our results would not be biased by using an over-weighted or a skinny model. The original non-pregnant woman model weighs 75.5 kg for a height of 1.74 m, which corresponds to a Body Mass Index (BMI) of 24.9, which contains 3.46 kg of subcutaneous abdominal fat. This amount of fat remains constant during the pregnancy.

2.1.2. From 8 to 13 WA: fetus models developed from ultrasound images. For fetus models during the first trimester of pregnancy, we used embryo/fetus models generated from segmentation of ultrasound images (Dahdouh *et al* 2013, Anquez *et al* 2013). There was no specific image acquisition done for this study and we used data from routine acquisitions performed with the informed consent of subjects. Three UFUS were used, at: 8, 10 and 13 WA. Each embryo/fetus is composed of a fetal envelope and a brain. Figure 1 shows a 3D view of the trunks of the three developed 8 to 13 WA pregnant woman models.

2.1.3. From 14 to 32 WA: fetus models generated using a growth modeling tool. For fetus models during the second and third trimester of pregnancy, we used fetus models that were developed using a fetus growth modeling tool and MR images, allowing us to generate a

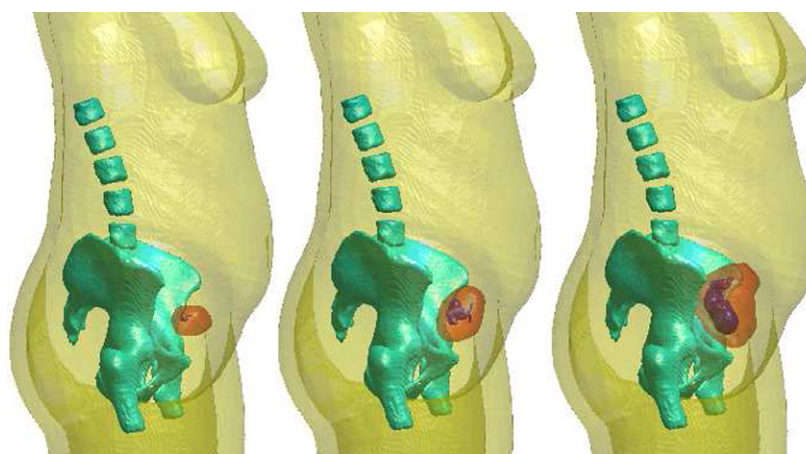


Figure 1. 3D views of the three developed pregnant woman models from respectively 8 to 13 WA using embryo/fetus models obtained from segmentation of Ultrasound images.

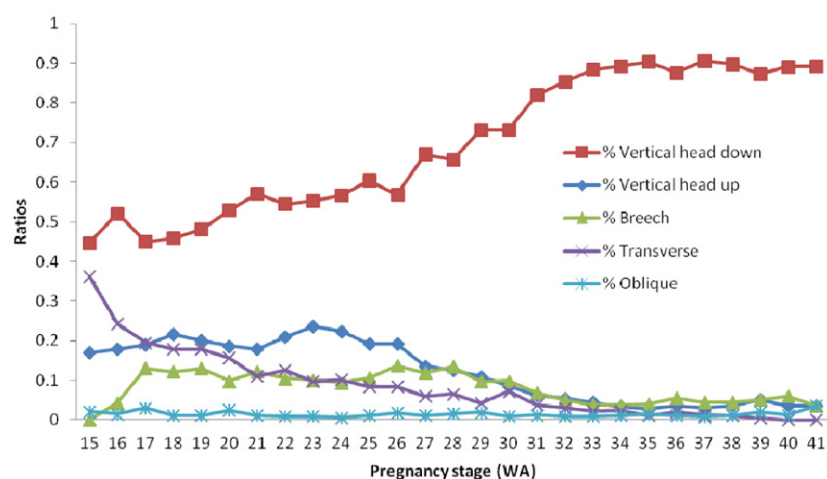


Figure 2. Percentages of occurrences of various fetal positions during pregnancy at stages between 15 and 41 WA, based on our image database.

model of the same fetus in the exact same position at different pregnancy stages (Serrurier *et al* 2013, Dahdouh *et al* 2014).

Using 17000 data obtained from ultrasound scans performed at the maternity of Port-Royal Cochin hospital, we derived statistics on the fetus position along a whole pregnancy (see figure 2). As we can observe in figure 2, during the whole pregnancy, a large majority of fetuses are in the vertical position, 40 to 90 % are head down and up to 20 % are head up. Breech, transverse or oblique positions are possible positions for the fetus until the end of the second pregnancy trimester but are more unlikely to happen at the last stage. We therefore decided to analyze the fetus exposure during a whole pregnancy in the vertical position with the head down or up.

Ten UFUS with a fetus in vertical position head down were generated from 14 to 32 WA, with 2 weeks increments. Each fetus is composed of the fetal envelope, the skull, the brain

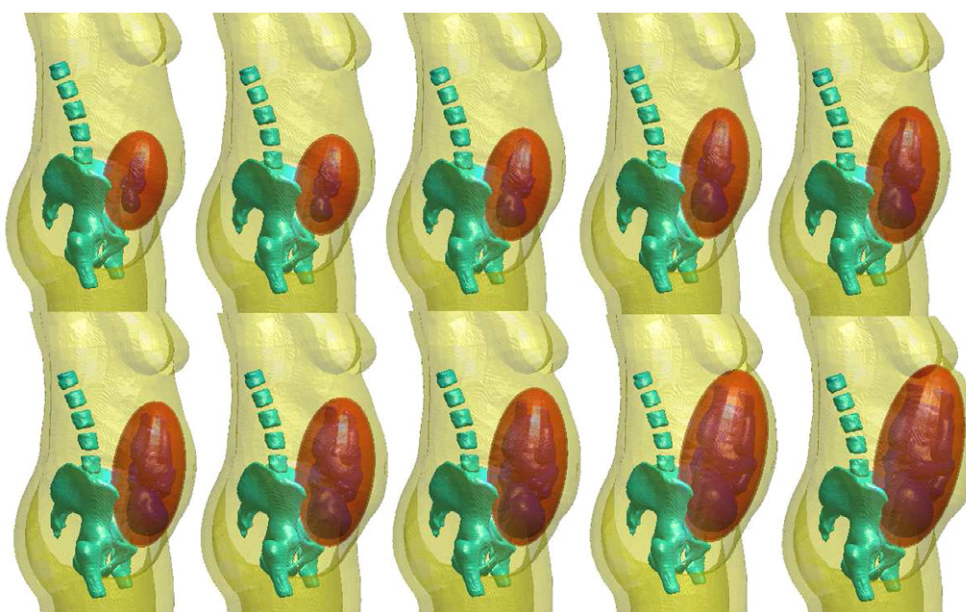


Figure 3. 3D views of the 10 developed pregnant woman models with the fetus in vertical position head down from 14 (left, top view) to 32 WA (right, bottom view) using fetus models generated using a fetus growth modeling tool.

and the lungs. The 10 UFUS were inserted in a synthetic semi-homogeneous pregnant woman body envelope. Figure 3 shows 3D views of the trunks of the 10 developed pregnant woman models.

Overall, 13 pregnant woman models were generated at a voxel resolution of 1 mm^3 . Each model is composed of the skin, subcutaneous abdominal fat and muscle, a pelvis bone, a UFU, including the uterus, the uterine content and the fetal tissues (envelope, skull, brain and lung), and finally, homogeneous tissues replacing all of the missing internal organs.

By simply rotating the fetus models inside the uterus, we developed 10 models of pregnant woman with a fetus in vertical position head up from 14 to 32 WA.

We calculated the weight of each fetus model by multiplying the number of voxels inside individual fetal structures by its density. Figure 4 compares weights of each fetus model with published data (Shinozuka *et al* 1987) of average weights of a fetus at the same pregnancy stage using fetal weight charts. We can see that weights of our generated fetuses are coherent with average fetal weights at the same pregnancy stages.

2.2. Setup of the fetal far-field exposure to EMF

The analysis was performed for fetuses in vertical position, head down or up.

While not overly realistic, subcutaneous fat was considered to be constant throughout pregnancy. Indeed, since it is very difficult to predict the evolution of subcutaneous fat for a given woman during the pregnancy, we decided to maintain the initial subcutaneous fat throughout pregnancy. Therefore, dosimetry results for later pregnancy stages when the pregnant woman is supposed to gain fat are likely to be a bit overestimated when given the influence of the subcutaneous abdominal fat layer on the fetal exposure.

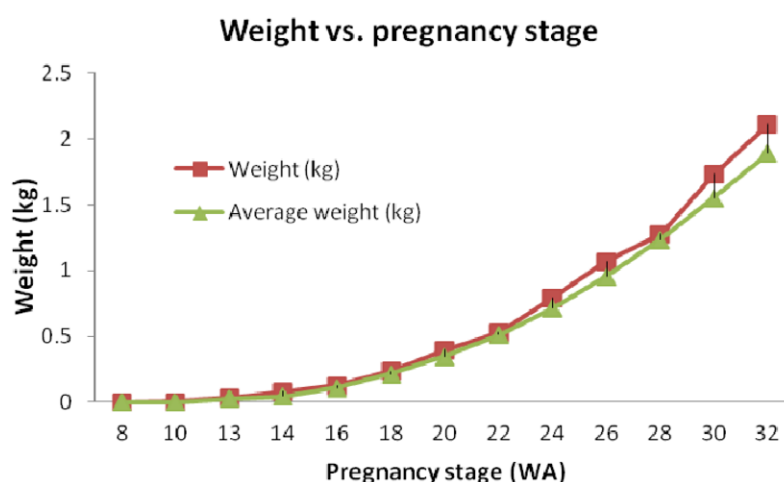


Figure 4. Comparison of generated fetus weights and average fetal weights at the same pregnancy stages.

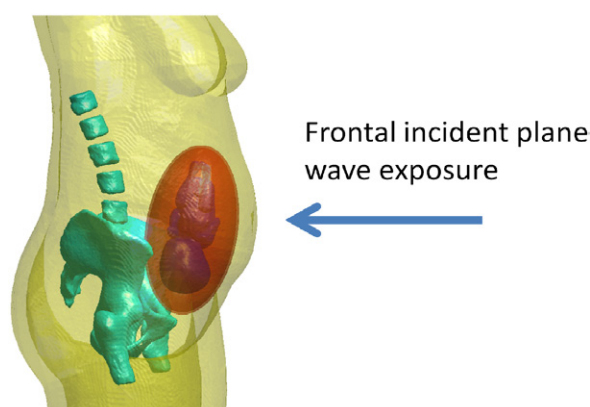


Figure 5. Direction of arrival of the incident plane wave.

We simulated a far-field exposure of the 13 different numerical models of a pregnant woman simulating the different stages of a pregnancy using an incident plane wave polarized vertically, with a frontal incidence, emitting at the frequency of 2100 MHz (Incident E-field $E = 1 \text{ V m}$) (see figure 5). All of the pregnant woman models were truncated to keep only the upper body for the simulations in order to reduce prohibitive calculation times (from a few days when using the whole pregnant woman body to a few hours when using only the upper body) and also because we were only interested in the fetus exposure. The impact of this truncation will be investigated in the following.

The well-known Finite Difference Time-Domain (FDTD) method (Taflöv 2000) is used to evaluate the total power absorbed by the fetus inside the different pregnant woman models and to evaluate the Specific Absorption Rate (SAR) distributions.

The dielectric properties of skin, muscle, bones and fat in the adult body were taken from (Gabriel 1995, Gabriel *et al* 1996a, Gabriel *et al* 1996b, Gabriel *et al* 1996c). The dielectric properties of the homogeneous tissue replacing all of the internal organs and tissues were

Table 1. The tissues' dielectric properties and the densities used in the study.

| Tissue | Permittivity <i>F/m</i> | Conductivity <i>S/m</i> | Density <i>kg m⁻³</i> |
|---------------------------|----------------------------|----------------------------|-------------------------------------|
| Fetal brain | 62.5 | 1.88 | 1020 |
| Fetal lungs | 34.80 | 1.08 | 722 |
| Fetal skeleton | 37 | 1.28 | 1650 |
| Fetal soft tissues | 59.3 | 1.89 | 1050 |
| Uterus | 58.4 | 1.97 | 1026 |
| Uterine content | 68.42 | 2.22 | 1007 |
| Woman fat | 5.31 | 0.08 | 916 |
| Woman muscle | 54.03 | 1.57 | 1047 |
| Woman homogeneous tissues | 14.64 | 0.45 | 1048 |
| Woman skin | 40.89 | 1.34 | 1125 |
| Woman pelvis | 15.276 | 0.50 | 1850 |

calculated by proportional averaging of dielectric properties of tissues surrounding the UFU (Jala *et al* 2013). It was assumed that the amniotic fluid has the same dielectric properties as the cerebrospinal fluid, as suggested in (Hand *et al* 2006). For the fetus's brain and bones dielectric properties, we used data specific to new born (Peyman *et al* 2001) and for the fetus's homogenized tissue we used data specific to fetuses (Peyman and Gabriel 2012). According to (Peyman and Gabriel 2012), no significant difference between dielectric properties of fetal homogenized tissue at different stages of pregnancy is observed. Thus, a unique value is used during the whole pregnancy. Table 1 shows the tissues' dielectric properties and the densities used in our study.

3. Results and discussion

3.1. Fetal exposure to EMF throughout pregnancy

At each pregnancy stage, we calculated the total power absorbed by the fetus ($P_{\text{abs}_{\text{fetus}}}$) and the ratio between the fetus whole-body SAR ($\text{WBSAR}_{\text{fetus}}$), normalized for an incident field $E = 61 \text{ V/m}$ (reference level at 2100 MHz), and the basic restriction in terms of whole-body SAR value ($\text{WBSAR}_{\text{limit}}$), as stated in the International Commission on Non-Ionizing Radiation protection (ICNIRP) guidelines (ICNIRP 1998). Our results are shown in table 2. Globally, the total absorbed power increases with the fetus weight and, consequently, with the pregnancy stage. We can remark that, whatever the pregnancy stage, the fetus normalized whole-body SAR is below the basic restriction of 0.08 W kg^{-1} . Although the values at 8 and 10 WA are particularly higher, one may ask the relevance of comparing values obtained for fetuses weighing only a few grams with whole-body basic restrictions.

We also calculated the average SAR values in the fetus brain and maximum averaged SAR over 1 g of brain tissues (from 14 WA as fetus weights at early stages are too small). Epidemiological studies analyzing the hypothetical relationship between the EMF exposure and cancers are particularly focused on brain tumors and accordingly, on the brain cumulative exposure to EMF (Cardis *et al* 2011, Cardis *et al* 2011, Aydin *et al* 2011). We, therefore, put a particular effort into characterizing the exposure of the fetus brain to EMF.

The variations of SAR values during the whole pregnancy are illustrated in figure 6.

In figure 6, we can first remark that variations of average SAR in the fetus brain and fetus whole-body SAR values are similar. During the first trimester of pregnancy the SAR values vary greatly, decreasing during the first trimester, and varying very little during the second and third trimesters. The decrease during the first trimester can be explained by the high variations of the

Table 2. Total fetus absorbed power (for an incident field $E = 1 \text{ V/m}$) and ratio between the fetus whole-body SAR normalized for an incident field $E = 61 \text{ V/m}$ and the basic restriction in terms of whole-body SAR value at each pregnancy stage.

| | | | | | | |
|---|----------------------|----------------------|----------------------|----------------------|----------------------|----------------------|
| Pregnancy stage (WA) | 8 | 10 | 13 | 14 | 16 | 18 |
| Fetus weight (kg) | 0.00036 | 0.0049 | 0.034 | 0.082 | 0.127 | 0.236 |
| Fetus brain weight (g) | 0.08 | 0.9 | 5.2 | 7.7 | 17.7 | 41.3 |
| $P_{\text{abs}}_{\text{fetus}}$ (mW) | 5.4×10^{-6} | 4×10^{-5} | 1.4×10^{-4} | 1.2×10^{-4} | 2.7×10^{-4} | 4.3×10^{-3} |
| $\text{WBSAR}_{\text{fetus}}/\text{WBSAR}_{\text{limit}}$ | 0.7 | 0.37 | 0.2 | 0.07 | 0.1 | 0.08 |
| Pregnancy stage (WA) | 20 | 22 | 24 | 26 | 28 | 30 |
| Fetus weight (kg) | 0.3972 | 0.529 | 0.7912 | 1.07 | 1.28 | 2.11 |
| Fetus brain weight (g) | 80.8 | 81.5 | 87.7 | 99 | 142 | 236 |
| $P_{\text{abs}}_{\text{fetus}}$ (mW) | 7.7×10^{-4} | 9.7×10^{-4} | 2.5×10^{-3} | 2.2×10^{-3} | 3×10^{-3} | 4.2×10^{-3} |
| $\text{WBSAR}_{\text{fetus}}/\text{WBSAR}_{\text{limit}}$ | 0.09 | 0.09 | 0.14 | 0.09 | 0.1 | 0.07 |

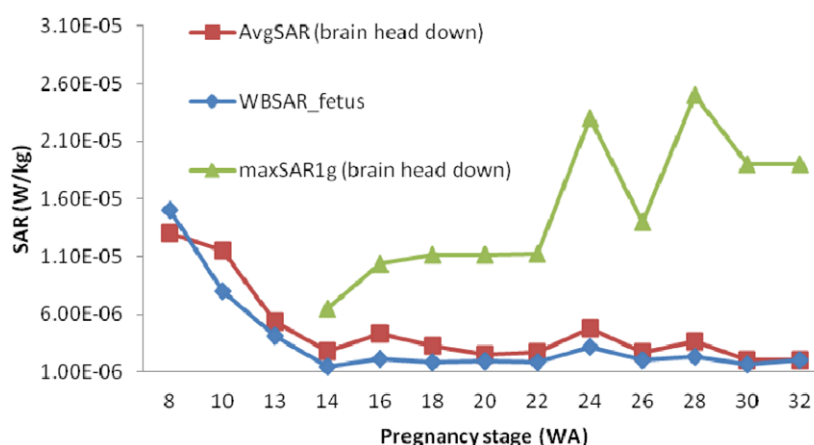


Figure 6. Variations of fetus whole-body SAR, average SAR, and maximum averaged SAR values over 1 g in the brain during the whole pregnancy.

fetus weight and the fetus brain weight: in 2 weeks both values can be multiplied by 10. Then, during the second and third trimesters the variations of the total power absorbed by the fetus and the fetus weight are quasi proportional, as shown in table 1, which shows that the fetus whole-body SAR varies only slightly during this period. The same trend is observed for the fetus brain.

For the maximum averaged SAR over 1 g of brain tissues values ($\text{maxSAR}_{1\text{g}}$), we can observe a jump between 22 and 24 WA. This corresponds to the tendency of the fetus around these stages to curl up inside the uterus, as we can see in figure 3 (this natural behavior is taken into account by the fetus growth modeling tool), because it starts to run out of space. Consequently, in the position we chose, the head gets closer to the mother’s abdominal

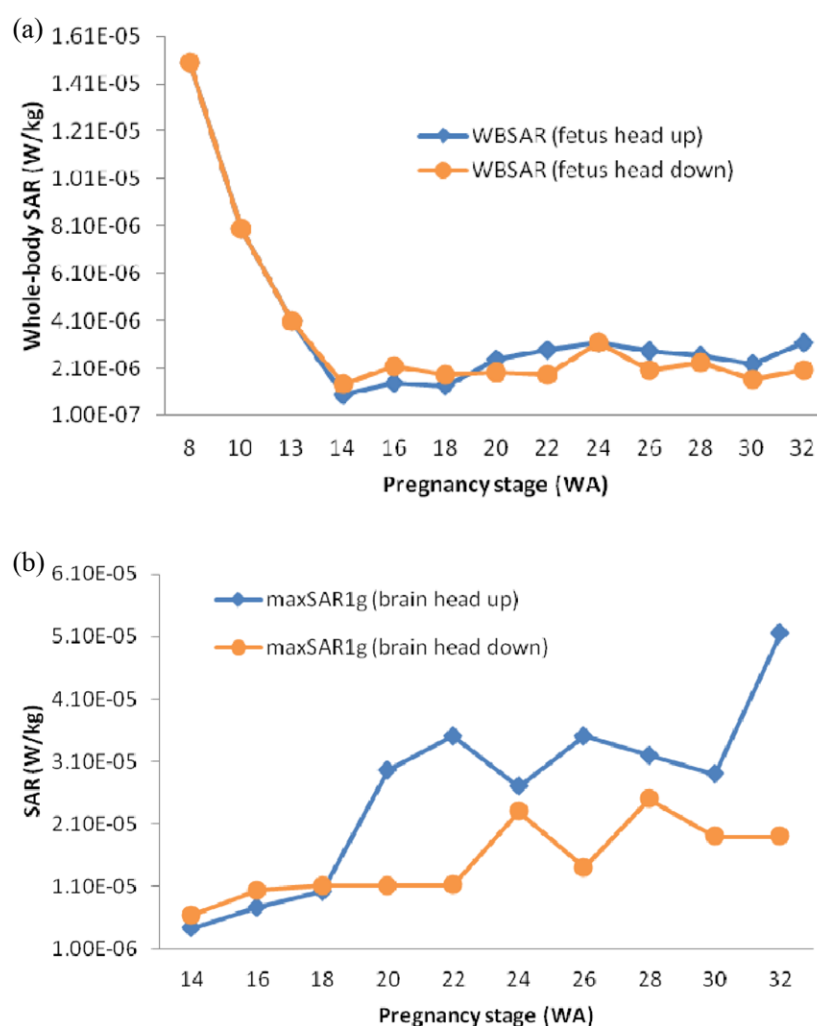


Figure 7. Comparison of whole-body (a) and local (b) exposures for a fetus in vertical position, head up and head down during the whole pregnancy.

surface and maxSAR1g values increase. Then, variations of maxSAR1g values (including the decrease between 24 and 26WA) can also be explained by the way the growth modeling tool is generating the UFU, building an egg-shaped uterus around the convex envelope of the fetus. Just a few more millimeters between the fetus head and the abdominal surface are enough to induce a sharp increase or decrease of maxSAR1g values.

3.2. Influence of the fetus position on the whole-body and local maximum exposure of the fetus during the whole pregnancy

A similar analysis was performed for fetuses in a vertical position with the head up. The variations of whole-body SAR values and local SAR values along the whole pregnancy were very similar to the variations observed for fetuses in a vertical position with the head down, as shown in figure 7. The 8, 10 and 13WA models were included in the whole-body SAR

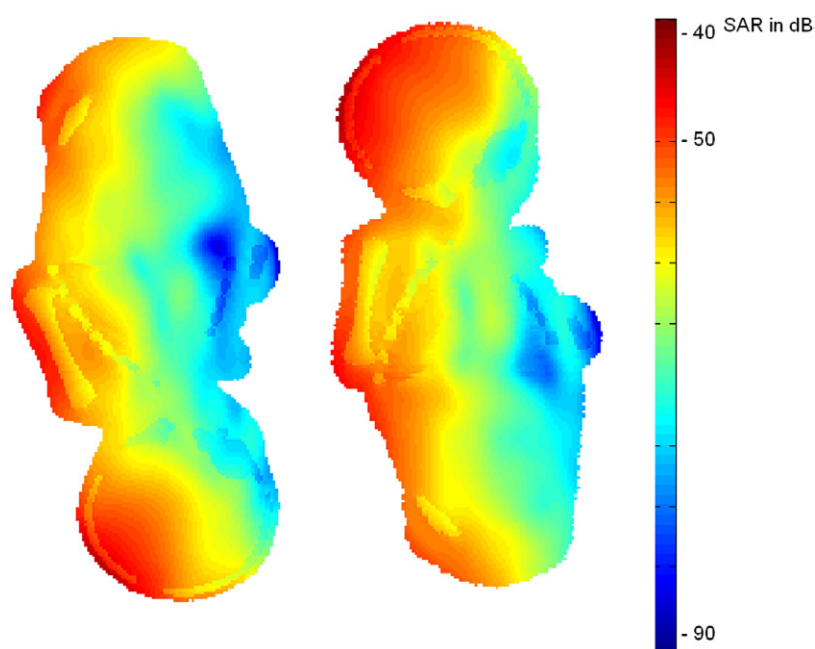


Figure 8. SAR distribution in 28WA fetuses in positions with the head down on the left and the head up on the right.

analysis without rotating the fetus because it is difficult, at these stages, to distinguish the different body parts.

We also compared the fetus whole-body and local exposures in a vertical position with the head up or down at each pregnancy stage.

We can observe in figure 7(a) that the behavior of the fetus whole-body SAR for a fetus with the head up is similar to the behavior for a fetus with the head down. From the second trimester, there are very few variations in the whole-body SAR.

If we compare the fetus exposure for the two positions, both whole-body SAR and max-SAR_{1g} values tend to be a bit higher for the fetus with the head up, as illustrated in figure 7 and figure 8. The exposure of the fetus therefore appears to depend on its position: for a frontal plane wave exposure, the head of the fetus gets more exposed when the fetus is with the head up, as shown in figure 8. However, these results are to be interpreted with caution since they are specific to the UFU models we generated, and to the plane wave incidence and the frequency band that we chose.

3.3. Impact of female body truncation on dosimetry results

Simulations at 14, 24 and 32WA for fetuses in vertical position head down were also performed using the whole body pregnant woman model in order to characterize the uncertainties linked to the use of a truncated body.

Because in our study the amount of fat remains the same during the pregnancy, the weight of the pregnant woman model, excluding the fetus weight, does not change, which has consequences for a quasi constant whole body SAR of the mother during the pregnancy of 0.04 W kg^{-1} (normalized for an incident field $E = 61 \text{ V m}^{-1}$). The fetus whole body SAR was found to be on average 7 times less than the mother whole body SAR. This result

Table 3. Comparison between $P_{\text{abs}}_{\text{fetus}}$ and average SAR in the brain values obtained at three different pregnancy stages using a truncated pregnant woman model and the whole body model.

| Pregnancy stage | Whole body model | | Truncated model | |
|-----------------|--------------------------------------|---------------------------------------|--------------------------------------|---------------------------------------|
| | $P_{\text{abs}}_{\text{fetus}}$ (mW) | AvgSAR (brain) (W kg^{-1}) | $P_{\text{abs}}_{\text{fetus}}$ (mW) | AvgSAR (brain) (W kg^{-1}) |
| 14 WA | 1.05×10^{-4} | 2.00×10^{-6} | 1.18×10^{-4} | 2.78×10^{-6} |
| 24 WA | 2.26×10^{-3} | 3.8×10^{-6} | 2.52×10^{-3} | 4.8×10^{-6} |
| 32 WA | 4.03×10^{-3} | 1.56×10^{-6} | 4.23×10^{-3} | 2.02×10^{-6} |

seems to be consistent with results obtained in (Nagaoka *et al* 2008a, Dimbylow *et al* 2009, Hadjem *et al* 2010).

Table 3 compares the total power absorbed by the fetus and the average SAR in the fetus brain at three different pregnancy stages, both when using a truncated pregnant woman model and when using the whole body model. We can remark that the total power absorbed by the fetus when using the truncated pregnant woman body tends to be a bit overestimated (between 5 to 10 % of overestimation) when compared to the values obtained when using the whole body pregnant woman model. This overestimation was expected because the truncated parts removed from the body are absorbing a non-negligible part of the received power, which has consequences for a smaller exposure of the fetus in the case of use of the whole body of the pregnant woman model. Since we were interested in comparing the exposure of the fetus between different pregnancy stages and different positions of the fetus, we can consider that small possible variations between 5 to 10 % of the calculated fetus absorbed power values with the truncated pregnant woman models have a little impact or no impact, on our analysis. As of our comparison with basic restrictions, since the values are overestimated with truncated models, our conclusions are expandable to results that would have been obtained with whole body pregnant woman models.

In terms of average SAR values in the fetus brain, we can see in table 3 that differences between values calculated with truncated pregnant woman models and values calculated with whole body pregnant woman models were higher than differences observed for the total power absorbed by the fetus. We could observe an overestimation when using truncated models ranging from 25 and 40 %. But, once again, since we were interested in comparing the exposure of the fetus brain during the pregnancy, these variations have a little impact on our analysis.

3.4. Discussion

In order to validate our results, we compared our calculated $\text{WBSAR}_{\text{fetus}}$ values with values obtained in (Nagaoka *et al* 2008a) with the same conditions of exposure (frontal plane wave at 2 GHz) at the same pregnancy stages. This comparison is summarized in table 4.

No discrepancies were found between the values that are of the same order of magnitude. Observed differences are certainly due to differences between the used pregnant woman and fetus models and also to the differences between the tissues and dielectric properties considered in both studies.

Concerning the very little variations of the fetus whole-body SAR during the second and the third pregnancy trimesters, the conclusions of the authors in (Nagaoka *et al* 2008a) were that the fetus whole-body SAR varies slightly with the pregnancy stage and that we could presume that the pregnancy stage can affect the exposure of the fetus. Nevertheless variations of the fetus whole-body SAR between the three different considered pregnancy stages in (Nagaoka *et al* 2008a) were very small, whatever the frequency band, and our results confirm

Table 4. Comparison between $\text{WBSAR}_{\text{fetus}}$ obtained at three different pregnancy stages in (Nagaoka *et al* 2008a) and in our study for a frontal plane wave exposure at 2 GHz.

| Pregnancy stage | Fetus weight | $\text{WBSAR}_{\text{fetus}}$ ($E = 61 \text{ V m}^{-1}$) |
|---|--------------|--|
| (Nagaoka <i>et al</i> 2008a) 12 weeks pregnancy | 66.6 g | 0.015 W kg^{-1} |
| 14 WA | 82 g | 0.006 W kg^{-1} |
| (Nagaoka <i>et al</i> 2008a) 20 weeks pregnancy | 542 g | 0.015 W kg^{-1} |
| 22 WA | 529 g | 0.007 W kg^{-1} |
| (Nagaoka <i>et al</i> 2008a) 26 weeks pregnancy | 1248.2 g | 0.01 W kg^{-1} |
| 28 WA | 1280 g | 0.008 W kg^{-1} |

that during the second and third trimesters of pregnancy there are very few variations of the fetus exposure in terms of whole-body SAR.

Although our study was performed at the 2.1 GHz frequency, our results should be quite similar for different frequency bands. Indeed, in (Nagaoka *et al* 2008a), only little variations of the fetus whole body SAR with the pregnancy stage were observed, whatever the frequency band, which would let us suppose that we would obtain the same kind of results at other frequencies for the fetus whole body SAR. In (Hadjem *et al* 2010), at 900 MHz with different fetuses (not the same fetus evolving with age and not in the same position) at different pregnancy stages, the variations of the fetus whole body SAR are not so important, which would reinforce our hypothesis that we should have the same kind of behavior of the fetus whole body SAR whatever the frequency.

Our observations and drawn conclusions for the fetus brain exposure during the pregnancy can be considered as new material for epidemiological studies looking at the possible correlation between the exposure to EMF and the risk of brain tumors, as well as for future studies of thermal modeling. A next step would be to consider using the different dielectric properties for the brain at different pregnancy stages given that the brain's composition evolves during the pregnancy (Moore *et al* 2011).

4. Conclusion

By analyzing the influence of the pregnancy stage on the environmental whole-body and local exposure of a fetus in a vertical position with the head down in the 2100 MHz frequency band, we can conclude that during the first trimester of pregnancy both whole-body and average brain exposures of the fetus decrease while advancing in the pregnancy stage due to the rapid gain of weight of the fetus. From the beginning of the second trimester, the whole-body and the average brain exposures are quite stable because weight gains (whole fetus and brain) are quasi proportional to the absorbed power increase. This behavior is different for the maximum averaged SAR value over 1 g in the brain. The $\text{maxSAR}_{1\text{g}}$, after the 22 WA, tends to increase because the fetus is running out of space and naturally curls up inside the uterus, which brings the head closer to the abdominal surface.

We have also studied the influence of the fetus position on its exposure. The behavior of the fetus whole-body and local exposures during pregnancy for a fetus in a vertical position with the head up was found of similar level, when compared to the position with the head down they were slightly higher, especially in the brain.

Acknowledgements

This work was performed in the framework of the project FETUS (<http://whist.institut-telecom.fr/fetus/>) co-funded by the Japan Science and Technology Agency (JST) and the

French National Agency for Research (ANR). We would like also to thank Dr Gilles Grangé from the maternity of Port-Royal Cochin hospital for statistics on the fetus position during the pregnancy, Professor C Adamsbaum and V Calmels at Bicêtre Hospital and G Captier at University Montpellier, for the imaging data we have used to build the models.

References

- Anquez J, Angelini E D, Grange G and Bloch I 2013 Automatic segmentation of ante-natal 3D ultrasound images *IEEE Trans. Biomed. Eng.* **60** 1388–1400
- Aydin D et al 2011 Mobile phone use and risk of brain tumours in children and adolescents: a multicenter case-control study (CEFALO) *J. Natl Cancer Inst.* **103** 1–16
- Becker J, Zankl M, Fill U and Hoeschen C 2008 Katja the 24th week of virtual pregnancy for dosimetric calculations *Pol. J. Med. Phys. Eng.* **14** 13–9
- Cardis E et al 2011 Risk of brain tumours in relation to estimated RF dose from mobile phones: results from five interphone countries *Occup. Environ. Med.* **68** 631–40
- Cardis E et al 2011 Exposure assessment: estimation of RF energy absorbed in the brain from mobile phones in the interphone study *Occup. Environ. Med.* **68** 686–93
- Dahdouh S, Serrurier A, Grange G, Angelini E D and Bloch I 2013 Segmentation of fetal envelope from 3D Ultrasound images based on pixel intensity statistical distribution and shape priors *IEEE International Symposium on Biomedical Imaging: From Nano to Macro ISBI'13*
- Dahdouh S, Varsier N, Serrurier A, De la Plata J P, Anquez J, Angelini E D, Wiart J and Bloch I 2014 A comprehensive tool for image-based generation of fetus and pregnant women mesh models for numerical dosimetry studies *Phys. Med. Biol.* **59** 4583
- De la Plata Alcalde J-P, Bibin L, Anquez J, Boubekeur T, Angelini E D and Bloch I 2010 *Physics-based modeling of the pregnant woman* Lecture Notes in Computer Science **5958** 71–81
- Dimbylow P 2006 Development of pregnant female, hybrid voxel-mathematical models and their application to the dosimetry of applied magnetic and electric fields at 50Hz *Phys. Med. Biol.* **51** 2383–94
- Dimbylow P J, Nagaoka T and Xu X G 2009 A comparison of foetal SAR in three sets of pregnant female models *Phys. Med. Biol.* **54** 2755–67
- Gabriel C 1995 Compilation of the dielectric properties of body tissues at RF and microwave frequencies *Report prepared for the NRPB Microwave Consultants Ltd*
- Gabriel C, Gabriel S and Corthout E 1996a The dielectric properties of biological tissues: 1 literature survey *Phys. Med. Biol.* **41** 2231–49
- Gabriel S, Lau R W and Gabriel C 1996b The dielectric properties of biological tissues: 2 measurements in the frequency range 10 Hz to 20 GHz *Phys. Med. Biol.* **41** 2251–69
- Gabriel S, Lau R W and Gabriel C 1996c The dielectric properties of biological tissues: 3. Parametric models for the dielectric spectrum of tissues *Phys. Med. Biol.* **41** 2271–93
- Hand J W, Li Y, Thomas E L, Rutherford M A and Hajnal J V 2006 Prediction of specific absorption rate in mother and foetus associated with MRI examination during pregnancy *Magn. Reson. Med.* **55** 883–93
- Hadjem A, Conil E, Anquez J, Bibin L, Angelini E D, Bloch I and Wiart J 2010 Analysis of the SAR induced in the fetus at different stages of gestation exposed to plane wave at 900 MHz *Bioelectromagnetics Society (BEMS) Annual Meeting (Seoul, Korea June 2010)*
- ICNIRP Guidelines 1998 Guidelines for limiting exposure to time-varying electric, magnetic, and electromagnetic fields (up to 300 GHz) *Health Phys.* **74** 494–22
- Jala M, Conil E, Varsier N, Wiart J, Hadjem A, Moulines E and Levy-Leduc C 2013 Simplified pregnant woman models for the fetus exposure assessment *CR. Phys.* **14** 412–7
- Moore K, Persaud T and Torchia M 2011 *The developing human: clinically oriented embryology* (Philadelphia, PA: Elsevier)
- Nagaoka T, Saito K, Takahashi M, Ito K and Watanabe S 2008a Estimating specific absorption rates in pregnant women by using models at 12-, 20 and 26-weeks' gestation for plane wave exposures *EMC Europe 2008 Proc.* 1–4
- Nagaoka T, Saito K, Takahashi M, Ito K and Watanabe S 2008b Anatomically realistic reference models of pregnant women for gestation ages of 13, 18 and 26 weeks In *Proc. of 30th Annual Int. IEEE EMBC Conf.* 2817–20

- Nagaoka T, Togashi T, Saito K, Takahashi M, Ito K and Watanabe S 2007 Anatomically realistic whole-body pregnant-woman model and specific absorption rates for pregnant-woman exposure to electromagnetic plane waves from 10 MHz to 2 GHz *Phys. Med. Biol.* **52** 6731–43
- Peyman A and Gabriel C 2012 Dielectric properties of rat embryo and foetus as a function of gestation *Phys. Med. Biol.* **57** 2103–16
- Peyman A, Rezazadeh A A and Gabriel C 2001 Changes in the dielectric properties of rat tissue as a function of age at microwave frequencies *Phys. Med. Biol.* **46** 1617–29
- Serrurier A, Dahdouh S, Captier G, Calmels V, Adamsbaum C and Bloch I 2013 3D articulated growth model of the fetus skeleton, envelope and soft tissues *Innov. Res. Biomed. Eng.* **34** 349–56
- Shinozuka N *et al* 1987 Formulas for fetal weight estimation by ultrasound measurements based on neonatal specific gravities and volumes *Am. J. Obstet. Gynecol.* **157** 1140–5
- Taflove A 2000 *Computational Electrodynamics: The Finite-Difference Time-Domain Method* 2nd edition (Boston, MA: Artech House)
- Xu X G, Taranenko V, Zhang J and Shi C 2007 A boundary-representation method for designing whole-body radiation dosimetry models: pregnant females at the ends of three gestational periods—RPI-P3, -P6 and P9 *Phys. Med. Biol.* **52** 7023–44